IEEE Transactions on Nuclear Science, Vol. NS-26, No. 3, June 1979

DESIGN STATUS OF THE 2.5 GeV NATIONAL SYNCHROTRON LIGHT SOURCE X-RAY RING.*

S. Krinsky, L. Blumberg, J. Bittner, J. Galayda, R. Heese, J. C. Schuchman, and A. van Steenbergen†

Abstract

The present state of the design of the 2.5 GeV electron storage ring for the National Synchrotron Light Source is described. This ring will serve as a dedicated source of synchrotron radiation in the wavelength range 0.1 Å to 30 Å. While maintaining the basic high brightness features of the earlier developed lattice structure, recent work resulted in a more economical magnet system, simplified chromaticity corrections, and improved distribution of the X-ray beam lines. In addition, the adequacy of the dynamic aperture for stable betatron oscillations has been verified for a variety of betatron tunes.

Introduction

A 2.5 GeV electron storage ring is being designed for the National Synchrotron Light Source facility at Brookhaven National Laboratory. Storing 0.5 Amp at 2.5 GeV this ring will provide X-rays in the wavelength range 1-30 Å from the 12 KG bending magnets, and usable intensity down to 0.1 Å from superconducting wigglers located in the matched insertions. Fundamentally the lattice is that proposed by R. Chasman and G. K. Green[1] with small electron emittances resulting in high brightness optical sources. During the course of detailed design the symmetry of the lattice evolved from six-fold to eight-fold. This resulted in a reduction in the number and the cost of the magnetic elements, in a more favorable distribution of the X-ray beam lines on the experimental floor, and in an increase from three to five of the number of insertions available for wiggler magnets. The bend angle (22.5^{o}) of the dipole magnets is larger in the new structure than in the original six-fold lattice. Because of the greater bend angle the sextupole magnet downstream of the dipole no longer obstructs the X-ray beam line originating from the dipole center. The dispersion function at the positions of the sextupoles is increased relative to the original lattice, resulting in a decrease of the chromaticity correction sextupole strengths. The increased bend angle resulted in a somewhat larger electron emittance, but since its value is still very small this has been considered acceptable in the light of the advantages of the eight-fold structure.

One octant of the ring is sketched in Fig. 1. The gradient of the quadrupole QF is adjusted to make the arc achromatic, resulting in zero dispersion in the insertions. This implies that the operation of the wigglers will have a minimal effect on the damping properties of the ring. The gradients in the quadrupole triplets Q1, Q2, Q3 bounding the insertions can be adjusted to obtain the small values of β_x and β_y at the insertion center (IC) appropriate for wigglers with a small number of poles, or to obtain larger values of β needed for the operation of coherent wigglers. In Fig. 2 the β-functions and the dispersion η_x are plotted for a configuration having low-β insertions. The corresponding excitation strengths of the magnetic elements are given in Table I, and some important machine parameters are presented in Table II.

In order to perform experiments requiring high spatial resolution, it is necessary to have an X-ray source with high central brightness. A high brightness will result from the small damped emittance of the electron beam, $E_x=8\times10^{-8}$ m-rad and $E_y=8\times10^{-10}$ m-rad, assuming 10% coupling, and from the small values of the β-function at the X-ray source. The electron beam has a damped energy spread of $\sigma_\varepsilon/E=8\times10^{-4}$, and spatial half-widths $\sigma_x=(\beta_x E_x+\eta_x^2\sigma_\varepsilon^2/E^2)^{\frac{1}{2}}$ and $\sigma_y=(\beta_y E_y)^{\frac{1}{2}}$. The properties of the X-ray source at a typical location in the bending magnet and at the wiggler position are compared in Table III.

Table I. Magnetic Elements

Name	Type	Length	B,B', or B"*	Preceding Drift Length
IC	DRIFT	0		
Q1	QUAD	0.45 M	-12.64 T/M	2.25 M
Q2	QUAD	0.80	11.64 T/M	0.70
Q3	QUAD	0.45	-11.78 T/M	0.30
BB	DIPOLE	2.7	1.214 T	0.705
SD	SEXT	0.2	-256 T/M^2	0.80
SF	SEXT	0.2	160 T/M^2	0.70
QF	QUAD	0.45	10.79 T/M	0.15

*$B\rho$ = 83.5KG-M

Chromaticity Correction

For a ring with an even number of superperiods, the momentum dependence of the β-functions will be weakened if the tune change per superperiod[2] is near $(2n+1)/4$ with n being an integer. In accordance with this suggestion we have chosen an operating point with $\nu_x/8 \cong 1.21$ and $\nu_y/8 \cong 0.71$. The natural chromaticity $(pd\nu/dp)$ of the lattice is $\xi_x^o = -27$ and $\xi_y^o = -19$. Since the dispersion is zero outside of the arcs, the choice of location for the two families of chromaticity correction sextupoles is very limited. With the sextupoles in the positions as indicated in Fig. 1, the excitation strengths (B") needed to obtain a chromaticity of $\xi_x=\xi_y=+3$ are presented in Table I. Including the effects of the sextupoles, the momentum dependence of the betatron tunes and amplitude functions has been studied using the computer programs SYNCH[3] and PATRICIA[4]. The resulting nonlinear dependence has been found to be satisfactorily weak. The limiting amplitude of stable betatron oscillations has been studied from particle tracking using PATRICIA, and the resulting aperture is sufficient.

Injection

Injection into the X-ray ring will take place at an electron energy of 700 MeV. The single bunch circulating in the booster synchrotron will be transferred into one of the 30 buckets of the storage ring, and this operation will be repeated once per second. The design current of the booster is 20 ma, corresponding to 3.3 ma in the X-ray ring. Therefore, a charging time of several minutes is expected. Preceding the arrival of each bunch from the booster, the closed orbit will be brought near the septum, and the orbit bump will collapse before the injected particles make three revolutions. The septum is located on the inside of the ring,

* Research supported by the U.S. Department of Energy.

† National Synchrotron Light Source, Brookhaven National Laboratory, Upton, New York 11973.

0018-9499/79/0600-3806$00.75 © 1979 IEEE

in the triplet between the quadrupoles Q1 and Q2. The injected particles proceed in the direction away from the nearby insertion.

Table II. Machine Parameters

Energy range	0.7 GeV - 2.5 GeV	
Design current	1A (2.0 GeV) ($3.9\times10^{12}e^-$)	
	0.5A (2.5 GeV) ($1.9\times10^{12}e^-$)	
Circumference		170.08 M
Number of superperiods		8
Long straights		4.5 M
Dipole bending radius		6.875 M
Nominal tunes ν_x, ν_y		9.7, 5.7
Minimum β_x, β_y in long straights		1.4, 0.3 M
β_x, β_y at dipole center		0.8, 14.0 M
Maximum β_x, β_y		26, 28 M
Maximum dispersion η_x		1.4 M
Momentum compaction α		6.5×10^{-3}
Radiated power (0.5A at 2.5 GeV)		$252+9N_{WIG}$ (KW)
Orbital period		568 nsec
RF Frequency (harmonic number)		52.88 MHz (30)
	0.7 GeV	2.5 GeV
RF peak voltage	50 KV	800 KV
Synch. oscillation period	0.38 msec	0.20 msec
Damping times $\tau_x \cong \tau_y$	0.26 sec	5.6 msec
τ_e	0.13 sec	2.8 msec
Energy aperture $\Delta E_{max}/E$	0.015	0.015
Energy spread σ_e/E	2.3×10^{-4}	8.2×10^{-4}
Natural bunch length $2\sigma_L$	5.4 cm	10 cm
Horizontal emittance	6.5×10^{-9}m-rad	8×10^{-8}m-rad

Instabilities and the Touschek effect are expected to be more severe at 700 MeV than at 2.5 GeV. A third-harmonic cavity is planned to reduce the microwave instability and to provide Landau damping against coupled bunch instabilities. Bunch lengthening and multiple scattering effects will tend to increase the Touschek lifetime, and a lifetime at 700 MeV of at least 30 min is expected. An effect important during acceleration is the generation of magnetic field perturbations due to eddy currents in the vacuum chamber. Calculation of the resulting tune shift suggest an acceleration time of approximately 3 min.

Beam Diagnostics and Correction

An rms quadrupole displacement error of 0.2 mm and an rms dipole rotation error of 0.5 mrad will result in an rms closed orbit displacement of Δx=12mm and Δy=13mm at a β-maximum. Beam position monitors will be placed at six positions per superperiod, each monitor determining both the horizontal and vertical position. The position monitors consist of pairs of "button electrodes" in the top and bottom of the vacuum chamber. Each of these electrodes is sequentially sampled by means of a tree of coaxial relays and converted to digital form. The relays are arranged so that the signals from the four electrodes at a single location are also available simultaneously for analog viewing. There are five horizontal and five vertical correction dipole magnets per superperiod. The maximum strength (BL) of an individual corrector is 64 G-M or 45 G-M depending upon its location. Calculations[5] indicate the feasibility of achieving a corrected orbit with a maximum deviation of 1 mm. In this case the vertical dispersion at the insertion center should be no greater than 1.5 cm, so we do not expect it to be necessary to correct the vertical dispersion separately.

Betatron tune measurements will be made by exciting betatron oscillations using an RF tickler, and the regular position pick-up electrodes at a single location will serve as a detector. The possibility of including the pick-up electrodes and the RF tickler in a closed loop of variable gain will be investigated with the goal of continuously monitoring the tune while exciting oscillations of only small amplitude. A toroidal beam transformer will be used to monitor the intensity of the circulating beam. Beam intensity, position, and fast bunch structure will also be monitored by observing the visible part of the synchrotron radiation at one azimuthal location.

Vacuum System

The vacuum chamber will be fabricated from an aluminum extrusion, alloy 6063-T5. An aluminum extrusion was chosen over a fabricated stainless steel chamber because: (1) it makes possible a design that minimizes changes in chamber cross-section that tend to excite RF losses, (2) it simplifies the cooling by incorporating cooling channels in the extrusion, and (3) aluminum is an excellent UHV material having a low outgassing rate after conditioning. Argon glow discharge conditioning is planned to reduce the gas desorption coefficient below the value achieved after bake-out. Where possible the chambers will be welded together in-situ, to reduce the number of flanged joints. Aluminum to stainless steel transition material will be used to join stainless steel flanges and bellows to the chamber. Distributed ion pumps will be used in all bending magnet chambers. In order to increase the pumping speed downstream of the bending magnets conventional sputter-ion pumps will be used, and provision will be made for installing titanium sublimation pumps. Cooling of the general run of the chamber is via two water channels in the extrusion. (Fig. 3) To allow the X-radiation to pass into the experimental beam-line, a slot is cut between the

Table III. Experimental Parameters

Energy E = 2.5 GeV, Current I = 0.5 Amp

	Dipole	Wiggler
Magnetic Field	1.2 T	4.0 T
Critical Wavelength	2.5 Å	0.74 Å
$4\sigma_x$	1.6 mm (typical)	1.3 mm
$4\sigma_y$	0.5 mm (typical)	0.06 mm
$N_\gamma(\lambda)$(ph/s/mrad/1% $\Delta\lambda/\lambda$)	3.2×10^{13} (λ=1Å)	1.0×10^{12} (λ=0.1Å)
	2.5×10^{14} (λ=10Å)	2.2×10^{13} (λ=0.2Å)
	6.0×10^{13} (λ=4000Å)	2.2×10^{14} (λ=1.0Å)

two channels. At the corner at the downstream end of the slot, there is normal incidence of the synchrotron radiation, and a water cooled copper block will be used in place of the aluminum extrusion which would melt.

References

1. R. Chasman and G. K. Green, in the Proposal for a National Synchrotron Light Source (BNL 50595); R. Chasman, G. K. Green and E. M. Rowe, IEEE Transactions on Nuclear Science, NS-22, 1765 (1975).
2. R. W. Chasman, E. D. Courant, and M. Month, IEEE Transactions on Nuclear Science, Vol. NS-22, 1429 (1975).
3. SYNCH written by A. A. Garren and A. S. Kenney.
4. PATRICIA written by H. Wiedemann.
5. We have used the computer program CLSORB written by G. Parzen and K. Jellett.

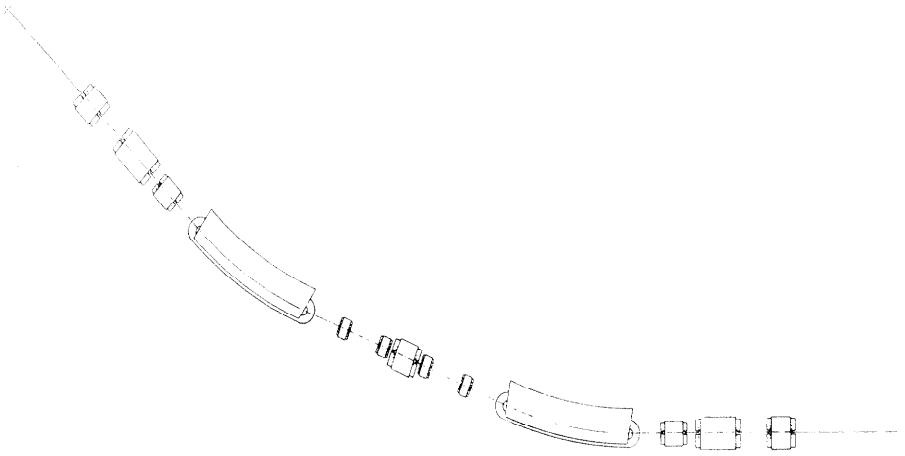

Fig. 1. One octant of the ring.

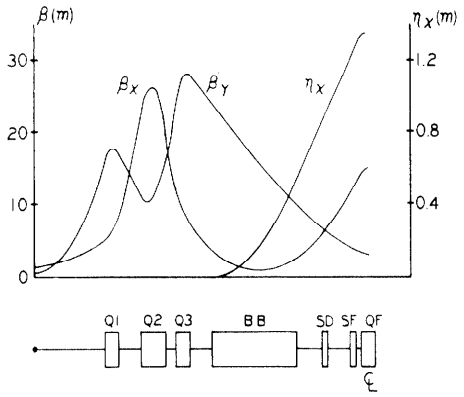

Fig. 2. Amplitude functions $\beta_{x,y}$ and dispersion η_x.

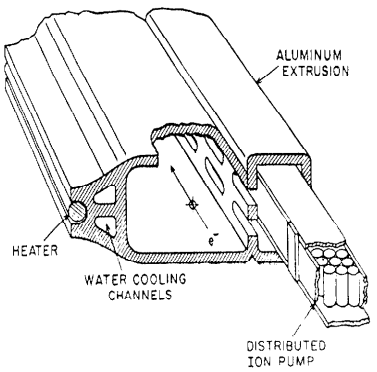

Fig. 3. Vacuum chamber.